RECEIVED BY TIC NOV - 7 1977

Presented at the Symposium on the Production and Neutralization of Negative Hydrogen Ions and Beams, Brookhaven National Laboratory, Upton, LI, New York, September 26-30, 1977

LBL-6839

CONF-770940-8

MASTER

Energy and Environment Division

D^- Production By Backscattering From Clean Alkali-Metal Surfaces

P.J. Schneider, K.H. Berkner, W.G. Graham, R.V. Pyle and J.W. Stearns

September 1977

Lawrence Berkeley Laboratory University of California/Berkeley

Prepared for the U.S. Energy Research and Development Administration under Contract No. W-7405-ENG-48

LBL-6839

DISTRIBUTION OF THIS DOCUMENT IS UNLIMITED

NOTICE
This report was prepared as an account of work sponsored by the United States Government. Neither the United States nor the United States Energy Research and Development Administration, nor any of their employees, nor any of their contractors, subcontractors, or their employees, makes any warranty, express or implied, or assumes any legal liability or responsibility for the accuracy, completeness or usefulness of any information, apparatus, product or process disclosed, or represents that its use would not infringe privately owned rights.

D^- PRODUCTION BY BACKSCATTERING FROM CLEAN ALKALI-METAL SURFACES*

P. J. Schneider, K. H. Berkner, W. G. Graham, R. V. Pyle, and J. W. Stearns

Lawrence Berkeley Laboratory
University of California
Berkeley, California 94720

Abstract

Measurements have been made of the total backscattered D^- yields from Cs, Rb, K, Na and Li surfaces bombarded with D_2^+ and D_3^+ in the energy range 0.05 to 3.5 keV/nucleon. All measurements were made at a background pressure less than 10^{-9} Torr and the alkali-metal surfaces were evaporated onto a substrate in situ to assure uncontaminated surfaces. For each target, the D^- yield is at a maximum (as high as 12% per incident deuteron for Cs) between 150 and 300 eV/nucleon, and at any measured energy, the D^- yield decreases from Cs to Li in the order given above.

Introduction

Recent experiments have shown that it is possible to dramatically increase negative-ion yields from ion sources by adding an alkali metal to the discharge.[1,2] In H^- sources, the addition of Cs to the discharge has resulted in increases of more than an order of magnitude in the H^- current density.[3] Belchenko, Dimov and Dudnikov[3,4,5] and Hiskes, Karo and Gardner[6] have proposed models based upon surface production as the principal mechanism for H^- formation in these sources. Belchenko, Dimov and Dudnikov proposed that any hydrogen atom adsorbed on the surface has a high probability of residing as a negative ion and can be desorbed from the surface as a negative ion by an incident energetic particle from the discharge. Furthermore, the addition of Cs to the H^- source produces Cs coverage of the source surfaces; this lowers the surface work function, enhances the probability of escape without destruction of the negative ion from the surface, and increases the H^- yield. Hiskes, Karo and Gardner have hypothesized that H^- ions are formed in the collision of an energetic (1 to 100 eV) hydrogen atom with an adsorbed Cs atom. As the hydrogen atom approaches the Cs atom the interaction potential is of the sum of the image potential and the difference between the CsH and CsH^- molecular potentials. This interaction potential allows the transfer of an electron from the substrate to the hydrogen atom, which may escape from the surface as H^-.

H^- production from surfaces involves three processes: the reflection or desorption of the hydrogen from the surface, the formation of the negative ion at the surface, and the escape without destruction of the negative ion from the surface. In the mechanism proposed by Belchenko, Dimov and Dudnikov,[3,4,5] the probability of formation of the negative ion is unity and the probabilities of desorption and escape without destruction become the dominant factors in determining the negative-ion yield from the surface. In the partial-coverage model of Hiskes and Karo,[7] the probability of destruction of the negative ion is shown to be negligible, so that the probability of formation of the negative ion, along with the probability of reflection of the incident particle, become the dominant factors in determining the negative-ion yield from the surface.

These models have led to calculations of the H^- secondary emission coefficient (the number of negative ions emitted from the surface per incident nucleus) by Kishinevskii[8] and Hiskes and Karo[7]. Kishinevskii has estimated the H^- secondary emission coefficient to be 0.1 to 0.2 for particles leaving the surface with energies of tens of eV. Hiskes and Karo have calculated both formation and escape probabilities for surfaces with a partial monolayer coverage of Cs and have combined their results with those of Oen and Robinson[9], who have used a Monte Carlo technique to calculate the reflected fraction of the incident particles as a function of incident energy. In this way Hiskes and Karo predict H^- secondary emission coefficients of 0.5 to 0.3 over the backscattered-energy range 10 to 100 eV. Hiskes and Karo[7] have also calculated the escape probabilities from some thick alkali-metal surfaces.

There exist almost no experimental measurements for comparison with the above calculations. Therefore, we have undertaken the present experiment to measure the total backscattered D^- yields from low-work-function surfaces. In this experiment, thick alkali metal targets were used. Although fractional monolayer coverage would give even lower work functions, such surfaces are difficult to produce and to monitor. So, as a first step toward investigating surface processes in H^- ion sources, we have measured the backscattered D^- yields from thick, clean Cs, Rb, K, Na and Li surfaces bombarded by 0.05 to 3.5 keV/nucleon D_2^+ and D_3^+ beams.

*Work done under the auspices of the U. S. Energy Research and Development Administration

DISTRIBUTION OF THIS DOCUMENT IS UNLIMITED

Apparatus and Procedure

A beam of D_2^+ and D_3^+ ions was extracted from a hot filament discharge, accelerated to the desired energy, and momentum analyzed with a 30° bending magnet before entering the experimental chamber. The apparatus within the chamber (Fig. 1) was designed around two rectangular plates, perpendicular to the beam line; an aperture in the first plate (the collector) allowed the beam to pass through to the second plate (the target) from which D^-, D^0, D^+, e^- as well as sputtered particles were emitted. The collector was used to monitor the negative-ion current, therefore all other charged particles had to be prevented from reaching or leaving it: an electric field between the target and collector plates prevented positive secondary ions from reaching the collector and a transverse magnetic field suppressed secondary electrons. Also, an upbeam collimator shielded the collector from the primary beam. This collimator was the endplate of a Faraday cup (the collimator-Faraday cup) which was used to determine the total current incident onto the target: the total incident current was determined by the difference in current readings from the collimator-Faraday cup when the beam was deflected into the cup and when it was steered through the cup by a pair of upbeam deflection plates. The negative ion secondary emission coefficient (NISEC) was determined by taking the ratio of the collector current to the total incident current and dividing by the number of deuterons per incident molecular ion.

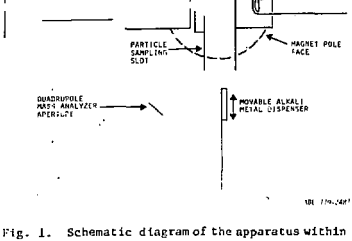

Fig. 1. Schematic diagram of the apparatus within the experimental chamber.

The collimator-Faraday cup, which was 2.5 cm in diameter, 4 cm long and had a 0.15-cm-diam exit aperture, was 0.08 cm upbeam from the collector.

The electric field used to suppress positive ions was produced by applying a negative voltage to the target. The magnitude of the applied voltage was determined by the beam species and energy. As an example, a 5.0-keV beam of D_3^+ required a target bias of at least −2.5 kV. The target bias adds to the incident energy giving a total incident energy of 7.5 keV; if we assume that the energy is divided equally between the three deuterons as the incident ion breaks up at the surface, then the maximum energy that a reflected D^+ ion can have is less than 2.5 keV, which is not sufficient for it to reach the collector plate. This explains why, in this experiment, only D_2^+ and D_3^+ were used as incident particles. For D^+ the maximum reflected energy is always greater than the retarding voltage, so that the high-energy backscattered D^+ ions cannot be prevented from reaching the collector.

The transverse magnetic field used to suppress secondary electrons from the target, the collector and the collimator-Faraday cup was produced by an electro-magnet with a 6.5-cm gap and 5-cm-diam poles. The suppression of secondary electrons is illustrated in Fig. 2, where the "apparent" NISEC is plotted vs the magnitude of the magnetic field. At low magnetic fields the signal is dominated by electrons, which are suppressed as the magnetic field is increased. For the case illustrated in Fig. 2 (3 keV/nucleon D_3^+, $|E_{gap}|$ = 4.6 kV/cm) 650 gauss is sufficient for complete electron suppression. Calculations of trajectories for D^- ions emitted from the target show that all negative ions (even those emitted with zero energy) reach the collector for all electric and magnetic fields used in this experiment.

Positive ions produced by backscattered particles (atoms and negative ions) striking the collector could not be suppressed in this experiment. The current due to these ions leaving the collector adds to the current from the collected negative ions and is a possible source of error. In appendix A we estimate that this effect contributes less than 5% to our NISEC measurements.

The target and collector plates were 7.3-cm high, 5-cm wide, and separated by 1.3 cm; the collector-plate aperture was 0.25 cm in diameter. To assure that all the negative ions produced at the target were collected, two separate tests were performed. The first test was to vary the effective width of the collector plate with a series of electrically isolated masks. The currents collected by the masks and by the collector were measured as a function of collector width. The ratio of the collector current to the sum of these currents remained constant at 0.99 for collector widths down to 3.6 cm and decreased as the collector width was further decreased. The second test was to vary the effective diameter of the aperture in the collector plate from 0.25 cm to 0.7 cm with another series of electrically isolated masks

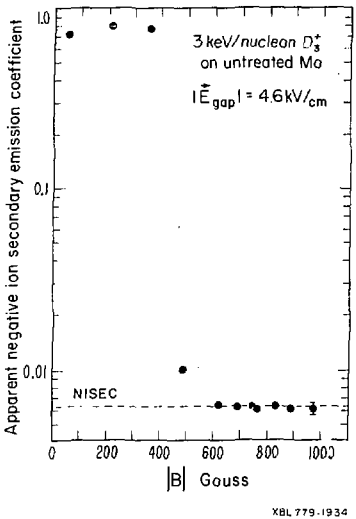

Fig. 2. Apparent NISEC vs the magnitude of the applied magnetic field for the case of 3 keV/nucleon D_3^+ on an untreated Mo target. The target bias was -6 kV, resulting in an electric field of 4.6 kV/cm.

which covered the collector plate. The ratio of the current on the mask to the current on the collector behind it was measured as a function of the diameter of the aperture. Extrapolation to zero diameter indicated that the loss of negative ions through the 0.25-cm-diameter aperture was (5 ± 5)%. From these tests, which were performed for incident energies from 0.75 to 3 keV/nucleon and with various electric and magnetic fields, we concluded that the dimensions of the collector plate were large enough, and the aperture small enough, to ensure that (95 ± 5)% of the negative ions were collected.

Clean alkali-metal targets were deposited on a substrate in the cryopumped experimental chamber, which was maintained at a pressure less than 10^{-9} Torr during the measurements. An S.A.E.S.† alkali-metal dispenser, mounted on a bellows, could be positioned between the target and collector plates to coat the target area. The thickness of the alkali-metal layer was determined by the current through the dispenser (6 to 8A) and the evaporation time. As an example, passing 7.5A through a Na dispenser for three minutes resulted in the emission of enough Na to form a layer about 15μm thick (assuming a Na sticking coefficient of unity), which is the same order of magnitude as the average penetration depth of a 7-keV/nucleon deuteron.[9]

Surface purity was monitored by mass analysis of positive and negative ions from the surface. An electrostatic-quadrupole mass analyzer, modified for either positive or negative ions, was placed in the chamber so that it sampled ions leaving the surface at an angle of 50° to the surface normal. Prior to evaporation, many different mass peaks were observed, indicating extensive surface contamination; after a thick alkali-metal target was deposited, the positive-ion spectrum showed only peaks corresponding to sputtered alkali-metal target ions and backscattered D^+ ions, while the negative ion mass spectrum showed only a D^- ion peak.‡ Thus, not only did we demonstrate the surface purity,‡ but also that the only negative ions from a clean surface were D^- - i.e. for clean surfaces, the measured NISEC is the D^- secondary emission coefficient. No change in the mass spectrum was observed for at least one hour after evaporation, demonstrating that the surface remained clean for this period of time.

For all except the Cs target, the measured NISEC remained constant for approximately one hour after the evaporation, then decreased at later times. This observation is consistent with the surface purity deduced from mass analysis. The NISEC measurement for Cs, on the other hand, decreased about 10% within about ten minutes after the evaporation, even though no impurities were observed by mass analysis. This suggests that either the NISEC for Cs is reduced by deuterium contamination (by the beam) of the surface or that small amounts of hydrogen, evolved from the Cs dispenser, reside upon the target surface and can be sputtered off as H^- to enhance the apparent NISEC.‡ In the latter case, the drop in the NISEC after about 10 min could be due to the removal of the hydrogen contamination of the surface, implying that the real NISEC for clean Cs would be about 10% lower than shown here. This anomaly is currently under investigation.

---

†SAES Getters/USA, Buffalo, New York.

‡In the presence of a large mass two peak, small amounts of mass one could not be resolved with the mass analyzer.

Results and Discussion

Figures 3 to 7 show the measured values of the NISEC for Cs, Rb, K, Na and Li targets as a function of the energy of the incident ions. The estimated standard uncertainties (±10%) indicated in the figures are the result of considering the effects discussed in the text (losses through the collector aperture and D^+ ions leaving the collector) as well as the calibration of the electrometers and reproducibility of the measurements. For Cs there may be an additional correction of -10% as previously discussed.

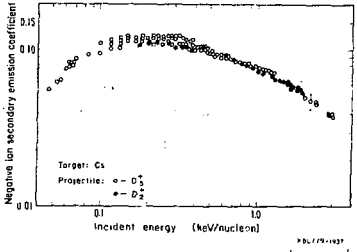

Fig. 3. NISEC vs incident energy for D_3^+ and D_2^+ incident on Cs (work function = 1.9 eV).

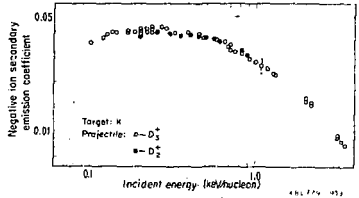

Fig. 5. NISEC vs incident energy for D_3^+ and D_2^+ incident on K (work function = 2.25 eV).

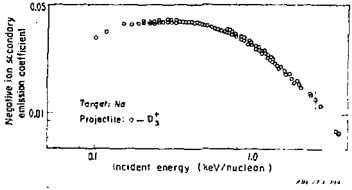

Fig. 6. NISEC vs incident energy for D_3^+ incident on Na (work function = 2.28 eV).

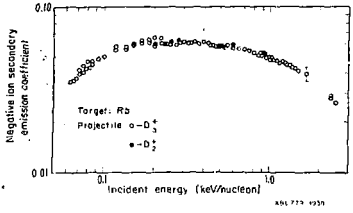

Fig. 4. NISEC vs incident energy for D_3^+ and D_2^+ incident on Rb (work function = 2.08 eV).

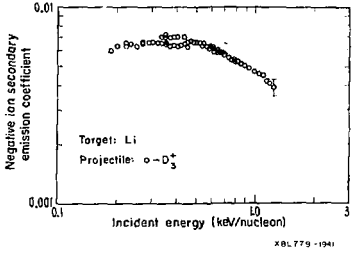

Fig. 7. NISEC vs incident energy for D_3^+ incident on Li (work function = 2.42 eV).

There are some features worth noting in Figs. 3 through 7:

(a) *All the targets show a maximum in the NISEC.*

(b) The value of the NISEC decreases in the order Cs, Rb, K-Na, and Li at any incident energy.

(c) The higher the maximum value of NISEC, the lower the incident energy at which it occurs.

(d) The NISEC is the same for either D_2^+ or D_3^+ ions.

We note that the ordering of the alkali metals given in (b) is according to increasing work function and decreasing target mass and atomic number.

To qualitatively understand H^- formation at surfaces, let us consider the processes described in the Introduction. For a given exit velocity the NISEC is the product of a formation probability (P_-) and a survival fraction (f) normalized to the number of incident nuclei (N_i). Since we are dealing with backscattered particles there is a distribution of exit velocities $R(v,\Omega)$. Thus

$$NISEC = \frac{1}{N_i} \int P_-(v,\Omega)\, f(v,\Omega)\, R(v,\Omega)\, dv d\Omega \qquad (1)$$

For the following discussion we assume that the terms are separable, so that

$$NISEC = R_N f P_- , \qquad (2)$$

where

R_N is the total reflection coefficient

P_- is the (averaged) probability of H^- formation, and

f is the (averaged) survival fraction as the H^- leave the surface.

Oen and Robinson[9] have shown that their calculated values of R_N result in a fairly universal curve for each incident-ion species, independent of the target, when plotted as a function of the reduced energy, ϵ.[5] This suggests that it is possible to make the R_N term in expression (2) target-independent to permit a comparison of fP_- for the five targets. Initially some preliminary NISEC results for 1.5 to 7.0 keV/ nucleon for H_3^+ incident ions on the alkali-metal targets (to be published) were plotted vs the reduced energy. While this was not particularly enlightening, it led to the discovery that when the NISEC was plotted as a function of ϵ/n_e (where n_e is the conduction-electron density of the target) a single curve, of the form

$$A \exp\left(-\alpha \sqrt{\epsilon/n_e}\right), \qquad (3)$$

could be obtained for Cs, Rb, K, and Na, but not for Li. Li could be fitted with the product of the same function and another function of the form:

$$1-\exp\left(-\beta \sqrt{\epsilon/n_e}\right). \qquad (4)$$

We note that n_e is proportional to the square of the plasma frequency of the electrons in the target and, therefore, may characterize the response time of these electrons to the perturbation of the incident ion. Furthermore, ϵ is proportional to the square of the velocity of the incident ion. Thus, $\sqrt{\epsilon/n_e}$ could be the characteristic interaction length.

Based upon these results, the NISECs for the alkali-metal targets bombarded with D_2^+ and D_3^+ were also plotted vs ϵ/n_e (Fig. 8). As can be seen from Fig. 8, all the curves can be fitted (within the experimental uncertainties) with a function of the form

$$A \exp\left(-\alpha \sqrt{\epsilon/n_e}\right) \left[1 - \gamma \exp\left(-\beta \sqrt{\epsilon/n_e}\right)\right], \qquad (5)$$

by adjusting only γ and β. This functional form implies that at higher values of ϵ/n_e these curves will coalesce to a simple exponential [see (3)].

The form (5) of the empirical fits to the NISEC curve is characteristic of the exponential-like dependences of formation and destruction processes involving electron tunneling through potential barriers. The first term could describe the electron tunneling from the surface to the atom (production). The exponential in the second expression could describe the electron tunneling from the atom back to the surface (destruction); the survival of the negative ion is thus given by (1-destruction) and has the form of expression (4).

It is encouraging to note that these functional forms are the same as those arrived at by Hiskes and Karo[7] in their calculations of the NISEC. When the empirical survival term (see the legend of Fig. 8) for a K surface was compared with the calculations of the survival fraction for a thick K surface done by Hiskes and Karo,[7] we found fairly good agreement. We would not expect exact agreement because their results are in terms of the exit energy and ours are in terms of the incident energy.

As a further step toward the understanding of partial coverage, we have monitored the NISEC as a function of the evaporation time for the targets Li and Na on a copper substrate. These results are shown in Figs. 9 and 10.

---

[5] The reduced energy is given by dividing the incident energy by the Lindhard energy, E_L, given by

$$E_L = \frac{Z_1 Z_2 e^2 (M_1 + M_2)(Z_1^{2/3} + Z_2^{2/3})^{1/2}}{a_o (0.8853) M_2}$$

where subscript 1 = projectile particles; subscript 2 = target particles; and a_o = Bohr radius, [J. Lindhard, M. Scharf and H. E. Schiott, Mat. Frys. Medd. Dan. Vied. Selsk., 33, No. 14 (1963)].

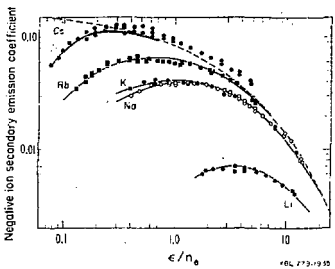

Fig. 8. NISEC vs ϵ/n_e for all five alkali-metal targets. ϵ is the reduced energy, $E_{incident}/E_L$, (see text) and n_e is the conduction-electron density of the targets, normalized to that of Li. The curves are empirical fits of the data to the function $A \exp(-\alpha\sqrt{\epsilon/n_e})\,[1-\gamma \exp(-\beta\sqrt{\epsilon/n_e})]$. The dashed curve is the asymptotic form common to all the targets: $A = 19.24$, $\alpha = 0.85$. The values obtained for γ and β are: Li - $\gamma = 1.14$, $\beta = 0.175$; Na - $\gamma = 1.26$, $\beta = 0.88$; K - $\gamma = 1.18$, $\beta = 0.85$; Rb - $\gamma = 1.45$, $\beta = 1.85$; and Ca - $\gamma = 4.18$, $\beta = 6.85$.

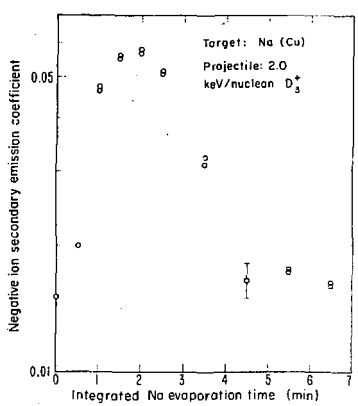

Fig. 9. NISEC for 2.0-keV/nucleon D_3^+ vs Na-evaporation time for Na deposited on a Cu substrate.

We expect that for thin coverages of several monolayers, the reflection coefficient (R_N) is characteristic of the substrate, while the work function is characteristic of the thin target material. Li and Na were chosen here because their R_N is much lower than that of the Cu substrate. We believe that even at the shortest evaporation times we have more than one monolayer coverage, but the work function of the deposited target material is not achieved until after a minute or two of deposition time (diffusion of contaminants from the substrate to the surface?). The initial rise in NISEC appears to be due to decreasing the work function while reducing R_N only a small amount. The subsequent decline over longer deposition times (thicker coatings) we attribute to the lower R_N of the deposited target materials.

In the case of Na on Cu, the peak value of the NISEC is a factor of four higher than for a thick Na target, while for Li the difference is an order of magnitude. No results are yet available for thin Cs coverage on various substrates, but investigations are currently being carried out using thin coverage of all the alkali metals and also using H_2^+ and H_3^+ incident on thick and thin alkali-metal surfaces.

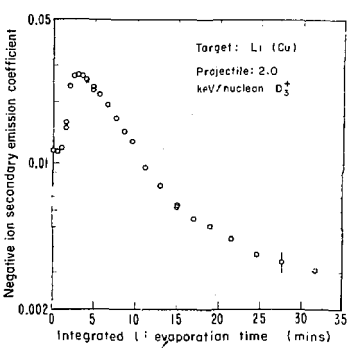

Fig. 10. NISEC for 2.0-keV/nucleon D_3^+ vs Li-evaporation time for Li deposited on a Cu substrate.

Acknowledgments

We gratefully acknowledge the support of H. A. Hughes, L. A. Biagi, and the members of their mechanical shops.

Appendix A

D^0 atoms and D^- ions may backscatter from the collector plate as D^+ ions and return to the target, giving an apparent NISEC larger than the true value:

$$\text{Apparent NISEC} = \text{NISEC} + \frac{\emptyset F_p}{\text{Incident nuclei/sec/cm}^2}$$

where $\emptyset$ = D^0 and D^- flux to collector plate from target

F_p = fraction of incident D^0 and D^- which are reflected as D^+.

To estimate an upper bound in the difference between apparent NISEC and NISEC, we need values for $\emptyset$ and F_p. $\emptyset$ is between 10% and 50% of the incident flux to the target.[9] From the results of Meischner and Verbeek[10] we infer that F_p is very small (~ a few percent) for the energies used in this experiment. To get a quantitative number, we made a mass analysis of positive and negative ions leaving an untreated Mo target. The ratio of D^- to D^+ leaving the Mo target at 70° to the normal is observed to be ≥ 10. The total D^- yield from the Mo target was 1% of the incident current, so the total D^+ yield is approximately 0.1%.

Untreated Mo and untreated stainless steel (the collector material) should have very similar properties in terms of reflected charge fractions; let us assume that they are the same. With F_p = 0.001, the observed NISEC is given by:

$$\text{Observed NISEC} = \text{NISEC} + \begin{Bmatrix} 0.50 \\ 0.10 \end{Bmatrix} \times 0.001$$

$$= \text{NISEC} + \begin{Bmatrix} 0.0005 \\ 0.0001 \end{Bmatrix}$$

Since the values of the NISEC are of the order of 0.01 - 0.1 for the alkali targets, the errors introduced in the NISEC measurements by D^+ emission from the collector plate are estimated to be less than 5%.

References

1. Yu. I. Belchenko, thesis, Institute of Nuclear Physics, Novosibirsk (1974).

2. R. Middleton, IEEE Trans. Nucl. Sci., 23, 1098 (1976).

3. Yu. I. Belchenko, G. I. Dimov and V. G. Dudnikov, Izv. Akad. Nauk SSSR Ser. Fiz. 37, 2573 (1973).

4. Yu. I. Belchenko, G. I. Dimov and V. G. Dudnikov, Zh. Tekh. Fiz., 45, 68 (1975) [Sov. Phys. - Tech. Phys. 20, 40 (1975)].

5. G. I. Dimov, presented at Second Symposium on Ion Sources and Formation of Ion Beams, Berkeley, Ca., 1974 .

6. J. R. Hiskes, A. Karo and M. Gardner, J. Appl. Phys., 47, 3888 (1976).

7. J. R. Hiskes and A. Karo, paper presented at this conference.

8. M. E. Kishinevskii, Institute of Nuclear Physics (Novosibirsk) Report IYAF 76-18 (1976).

9. O. S. Oen and M. T. Robinson, Proc. Second Conf. on Surface Effects in Controlled Fusion Devices, San Francisco, Ca., 1976, (North-Holland Publishing Company, Amsterdam, 1976), p. 210.

10. P. Meischner and H. Verbeek, J. Nucl. Mater., 53, 276 (1974), [Max-Planck-Institut fur Plasmaphysik Report IPP 9/18 (1975)].